# Vanoni MA, Curti B.. Structure-function studies of glutamate synthases: A class of self-regulated iron-sulfur flavoenzymes essential for nitrogen assimilation. IUBMB life 60: 287-3...

**ARTICLE** *in* INTERNATIONAL UNION OF BIOCHEMISTRY AND MOLECULAR BIOLOGY LIFE · MAY 2008

Impact Factor: 3.14 · DOI: 10.1002/iub.52 · Source: PubMed

IUBMB *Life*, 60(5): 287–300, May 2008

*Critical Review*

# Structure–Function Studies of Glutamate Synthases: A Class of Self-regulated Iron-sulfur Flavoenzymes Essential for Nitrogen Assimilation

**Maria Antonietta Vanoni and Bruno Curti**
*Dipartimento di Scienze Biomolecolari e Biotecnologie, Università degli Studi di Milano, Via Celoria 26, Milano, Italy*

*Summary*

**Glutamate synthases play with glutamine synthetase an essential role in nitrogen assimilation processes in microorganisms, plants, and lower animals by catalyzing the net synthesis of one molecule of L-glutamate from L-glutamine and 2-oxoglutarate. They exhibit a modular architecture with a common subunit or region, which is responsible for the L-glutamine-dependent glutamate synthesis from 2-oxoglutarate. Here, a PurF- (Type II- or Ntn-) type amidotransferase domain is coupled to the synthase domain, a $(\beta/\alpha)_8$ barrel containing FMN and one [3Fe-4S]$^{0,+1}$ cluster, through a ~30 Å-long intramolecular tunnel for the transfer of ammonia between the sites. In bacterial and eukaryotic GltS, reducing equivalents are provided by reduced pyridine nucleotides thanks to the stable association with a second subunit or region, which acts as a FAD-dependent NAD(P)H oxidoreductase and is responsible for the formation of the two low potential [4Fe-4S]$^{+1,+2}$ clusters of the enzyme. In photosynthetic cells, reduced ferredoxin is the physiological reductant. This review focus on the mechanism of cross-activation of the synthase and glutaminase reactions in response to the bound substrates and the redox state of the enzyme cofactors, as well as on recent information on the structure of the $\alpha\beta$ protomer of the NADPH-dependent enzyme, which sheds light on the intramolecular electron transfer pathway between the flavin cofactors.** 
IUBMB *Life*, 60(5): 287–300, 2008

**Keywords** nitrogen assimilation; amidotransferase; iron-sulfur clusters; flavoenzymes; enzyme activation; ammonia tunnel; glutamine; glutamate; intermediate channeling.

**Abbreviations** 2-IG, 2-iminoglutarate; 2-OG, 2-oxoglutarate; αGltS, α subunit of glutamate synthase; βGltS, β subunit of glutamate synthase; AS, asparagine synthetase; cryoEM, low temperature electron microscopy; CPS, carbamyl phosphate synthetase; DON, 6-diazo-5-oxo-L-norleucine; DPD, dihydropyrimidine dehydrogenase; $E_m$, mid-point potential; GltS, glutamate synthase; GlmS, glucosamine 6-phosphate synthase; FAD, flavin adenine dinucleotide; Fd, ferredoxin; Fd-GltS, ferredoxin-dependent glutamate synthase; FMN, flavin mononucleotide; GAT, glutamine amidotransferase; GS, glutamine synthetase; $K_M$, Michaelis constant; IGPS, imidazol glycerol phosphate synthase; L-Gln, L-glutamine; L-Glu, L-glutamate; MetS, L-methionine sulphone; NAD(P)H-GltS, NAD(P)H-dependent glutamate synthase; Ntn, N-terminal nucleophile; ONL, 5-oxonorleucine; PDB, protein data bank; PRPP-AT, phosphoribosyl pyrophosphate amidotransferase; SAXS, small angle X-ray scattering; SQD1, UDP-sulfoquinovose synthase; $V_{max}$, maximum velocity.

Received 7 January 2008; accepted 17 January 2008
Address correspondence to: Maria Antonietta Vanoni, Dipartimento di Scienze Biomolecolari e Biotecnologie, Università degli Studi di Milano, Via Celoria 26, 20133 Milano, Italy. Tel: +390250314901. Fax: +390250314895. E-mail: maria.vanoni@unimi.it

ISSN 1521-6543 print/ISSN 1521-6551 online
DOI: 10.1002/iub.52

## INTRODUCTION

Glutamate synthases (GltS) catalyze the reductive transfer of L-glutamine (L-Gln) amide group to the C(2) carbon of 2-oxoglutarate (2-OG). Peculiar features of GltS are (i) the ability to tightly couple the hydrolysis of glutamine and the addition of the released ammonia molecule to 2-OG, which take place at sites separated by 30 Å, through an intramolecular tunnel for ammonia transfer between the sites; (ii) a modular architecture, perhaps reflecting its evolutionary origin, which leads to three main GltS forms that share a common subunit (or domain) for the glutamine-dependent glutamate synthesis from 2-OG, but differ for the presence of a second subunit (or domain), which allows them to use reducing equivalents of reduced pyridine nucleotides as opposed to reduced ferredoxins (*1–4*).

Eubacteria contain a NADPH-dependent GltS (NADPH-GltS), which is formed by two different subunits (α subunit or αGltS, ~150 kDa, and β subunit or βGltS, ~50 kDa) closely associated to yield the catalytically active $\alpha\beta$ protomer. The latter contains one FAD (on βGltS), one FMN (on αGltS), and

three different iron-sulfur clusters (one $[3Fe\text{-}4S]^{0,+1}$ center and two different low potential $[4Fe\text{-}4S]^{+1,+2}$ clusters). Cyanobacteria and photosynthetic tissues of plants contain a ferredoxin-dependent GltS (Fd-GltS) formed by a single polypeptide chain similar to αGltS. The enzyme purified from yeast and nonphotosynthetic tissues of plants is formed by a single polypeptide chain derived from the fusion of the bacterial α and β subunits and was shown to be NADH-dependent. Genome sequencing projects revealed that NADH-GltS is also found in lower animals, including protozoa, (*e.g.*, *Plasmodium falciparum*), nematodes (*e.g.*, *Caenorhabditis elegans*), and insects (*e.g.*, *Aedes aegypti*, *Anopheles gambiae*, *Bombyx mori*, *Drosophila melanogaster)*. Among Chordata, an open reading frame encoding a putative GltS has only been found in the model organism *Ciona intestinalis*. In some of these organisms, the presence of glutamate synthase activity has also been demonstrated (*5–7*). In general, the eukaryotic GltS has been poorly characterized biochemically, but the similarity with the eubacterial NADPH-GltS suggests that they share structural and functional features.

In Archeae, it has been proposed that GltS is formed by the association of multiple subunits corresponding to some of the domains of the eubacterial, plant, and eukaryotic enzyme (*2, 8–10*). Whether in these organisms GltS is pyridine nucleotide- or ferredoxin-dependent is not known.

Studies on GltS initiated in the 70s when it was found that, in bacteria, it forms with glutamine synthetase (GS) a pathway, which efficiently assimilates ammonia when it is present at low intracellular levels (*11*). The GS/GltS pathway was also found in plants where mutants defective in Fd-GltS are invariably photorespiratory mutants revealing that Fd-GltS is important to reassimilate ammonia released during photorespiration, leaving to NADH-GltS a role in primary ammonia assimilation in roots (*10, 12*).

Because of the central role of glutamate in cell metabolism, GltS appears to be a valid target for the development of novel drugs and for metabolic engineering in, *e.g.*, the field of microbial bioconversions or improvement of crop production. For example, inactivation of the *glt*B and *glt*D genes, which encode the NADPH-GltS α and β subunit, respectively, led to a lethal phenotype in *Mycobacterium tuberculosis*, the causative agent of tuberculosis (*13*). NADPH-GltS has been implicated in the response to osmotic (*14*) and acid stress (*15*) and, recently, biofilm formation (*16*). Inactivation of the gene encoding NADH-GltS or interfering with its expression in *C. elegans* also leads to a lethal phenotype (www.wormbase.org) suggesting an essential role, in general, in lower animals, which include several pathogens (*e.g.*, helminths and *Plasmodia*) or pathogen vectors (*e.g.*, *Anopheles*, *Aedes*). Altered levels of GltS in, *e.g.*, yeast lead to modulation of NAD(P)H/$NAD(P)^+$ levels, a fact that can be exploited to optimize bioconversions [*e.g.*, (*17*)]. Furthermore, the enzyme has recently attracted attention as a marker of oxidative and nitrosative stress in bacteria (*18*), as a reference enzyme during studies of iron-sulfur cluster biogenesis (*19, 20*), or as a model system to develop advanced techniques for the study of protein structure (*21, 22*).

The exploitation of GltS in all these cases strictly depends on the understanding of its structural and catalytic properties, which mainly derive from studies on the GltS of *Azospirillum brasilense*, a nitrogen-fixing bacterium, taken as the model of the bacterial and eukaryotic NAD(P)H-GltS, and on the *Synechocystis* sp. PCC6008 Fd-GltS, the model of the plant enzyme.

Background information and references to earlier literature on GltS can be found in previous reviews (*1–4, 23*), whereas we will here focus on recent studies dealing with the mechanism of self-activation of the enzyme, also in relation to other amidotransferases, and on recent structural studies that led to the proposal of a molecular model of the NADPH-GltS holoenzyme. The amidotransferases have also been the object of several recent reviews (*24–30*). In the light of the rapidly growing body of literature on amidotransferases, we will mainly refer, quite arbitrarily, to the properties of just a few well-characterized amidotransferases, especially phosphoribosyl pyrophosphate amidotransferase (PRPP-AT), glucosamine 6-phosphate synthase (GlmS), and asparagine synthetase (AS), which share with GltS the PurF-type amidotransferase domain, also known as the Type II or Ntn-type glutamine amidotransferase (GAT) domain.

## THE MECHANISM OF GLUTAMATE SYNTHASE REACTION

The NADPH-GltS reaction consists of the six steps depicted in Fig. 1, top panel. Some, but not all, of the mechanistic details of the reaction have been elucidated.

The β subunit is a FAD-dependent NADPH oxidoreductase, which supplies FMN with the reducing equivalents needed for glutamate synthesis through at least two of the three GltS [Fe-S] clusters. Reductive glutamine-dependent glutamate synthesis takes place within αGltS.

The structure of αGltS in complex with the L-Gln analog L-methionine sulphone (MetS) and with the 2-OG substrate has been solved at 2.8 Å resolution [Fig. 2, (*31*)], and was soon followed by those of *Synechocystis* sp. PCC 6008 Fd-GltS alone, in complex with 2-OG or with 2-OG after reaction with 6-diazo-5-oxo-L-norleucine (DON) at the glutaminase site, which were solved at higher resolution (2.0–2.7 Å) (*23, 32, 33*). The αGltS and Fd-GltS are very similar to each other with respect to their sequence (45% identity) and three-dimensional structure, allowing us to extrapolate most of the information gathered on one of the protein species to the other. The glutaminase site is formed by the PurF-type (or Type II) N-terminal L-glutamine amidotransferase (GAT) domain (residues 1–422 in the αGltS). This fold is now known as the Ntn-type, from N-terminal nucleophile, since in these enzymes the acid-base catalysis is believed to be assisted by the free N-terminal amino group of the essential Cys(1) residue (*30*). At this site, the glutaminase reaction takes place. After binding, L-Gln is proposed to be hydrolyzed with the mechanism depicted in Fig. 1 lower panel (*30*). A water molecule may be bridging the Cys1 α-

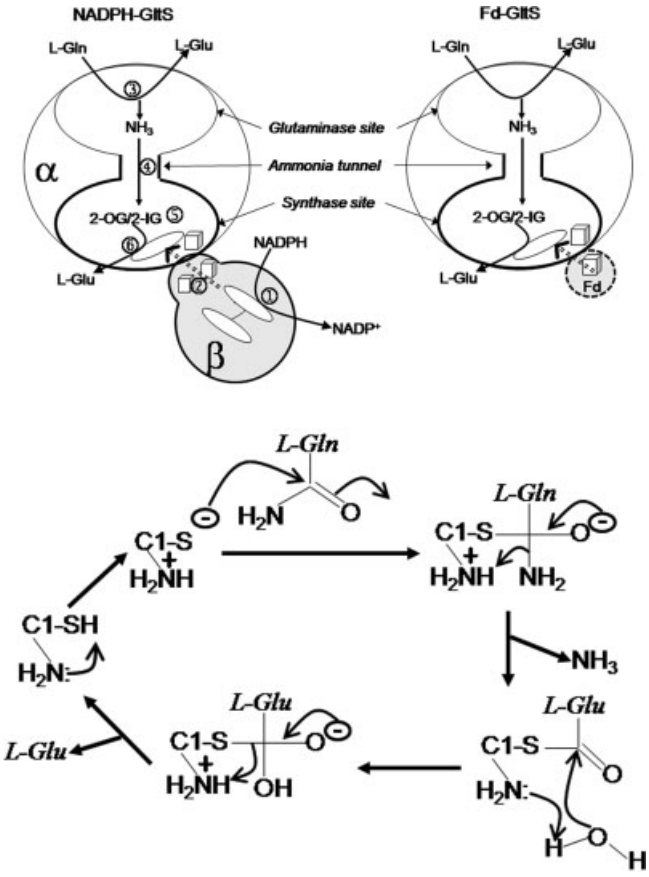


**Figure 1.** Glutamate synthase reaction. The glutamate synthase reaction occurring in NADPH-GltS is formally described as the sequence of 6 steps. Step 1: NADPH binding to $\beta$GltS and reduction of the FAD cofactor (two linked ovals); Step 2: electron transfer from FAD to FMN (oval) in the synthase domain of αGltS through the enzyme iron-sulfur clusters (cubes), namely: two low potential $[4Fe\text{-}4S]^{+1,+2}$ on $\beta$GltS and the $[3Fe\text{-}4S]^{0,+1}$ center on αGltS; Step 3: L-glutamine binding at the glutaminase site in the PurF-type glutamine amidotransferase domain and hydrolysis with release of the first L-glutamate product and ammonia; Step 4: ammonia transfer from the glutaminase to the synthase site through the intramolecular tunnel; Step 5: addition of ammonia to 2-OG bound to the synthase site with formation of the postulated 2-iminoglutarate (2-IG) intermediate; Step 6: reduction of 2-IG to L-Glu by reduced FMN. In Fd-GltS, reduced ferredoxin (Fd) is the electron donor. It has been shown that Fd binds to Fd-GltS with a 1:1 stoichiometry in solution, but also that the fully active enzyme is the reduced species in complex with reduced Fd (*33, 36*). The mechanism of the glutaminase reaction (step 3 in the top panel) is believed to occur as depicted in the lower panel, as proposed for all PurF-type amidotransferases. In these enzymes, also defined Ntn-type amidotransferases, the free N-terminal amino group participates in acid-base catalysis during the reaction.

amino and side chain thiol groups so that it may mediate proton exchange between the groups, as shown in (*25*).

As in the case of the growing family of well-characterized amidotransferases, in GltS a tunnel is present to transfer ammonia to the synthase site where the ammonia acceptor molecule is bound (*25, 26, 28, 30, 34*). In amidotransferases, the acceptor molecule undergoing amination or amidation is often phoshorylated (as in carbamyl phosphate synthetase (CPS), the prototype of the Triad class of amidotranferases,) or adenylated (as in AS, another Ntn-type amidotransferase). In other instances, ammonia adds to a carbonyl group yielding an imine intermediate, which evolves by cyclization (as in imidazol glycerol phosphate synthase, IGPS) or isomerization [as in GlmS, (*25*)]. In GltS, the reduction of the postulated 2-iminoglutarate (2-IG) intermediate drives the reaction. The latter reaction is referred to as the "synthase reaction." It takes place in the synthase domain of GltS, which is a $(\beta/\alpha)_8$ barrel, containing the FMN cofactor and the 2-OG binding site and sharing sequence and structural similarities with the family of FMN-dependent L-hydroxy acid oxidases and dihydroorotate dehydrogenase (*31*). The active site structure, the redox properties of the cofactors, and the direct observation of reduction of FMN by the L-glutamate product without formation of semiquinone species suggest that 2-IG reduction occurs by direct hydride transfer from the reduced FMN cofactor (*35, 36*). A surface loop of αGltS subunit (residues 1101–1118) carries the GltS $[3Fe\text{-}4S]^{0,+1}$ cluster, which has been shown to be a native component of the enzyme being readily reduced by reacting GltS with NADPH, the physiological electron donor (*37*). The location of the [3Fe-4S] cluster at the protein surface makes it available for electron transfer from the cofactors of the NADPH-GltS $\beta$ subunit (*31*) or from reduced Fd in Fd-GltS (*32, 33*).

The so-called central (residues 423–786) and C-terminal domain (residues 1204–1479) of αGltS appear to play structural roles acting as wedges that hold the glutaminase and synthase domains in place, allowing the formation of the ammonia tunnel.

The enzyme also catalyzes partial reactions, namely: (i) NADPH oxidation in the presence of synthetic electron acceptors (*e.g.*, iodonitrotetrazolium, ferricyanide, or dichlorophenolindophenol); (ii) the ammonia-dependent glutamate synthesis from 2-OG and ammonia (the so-called ammonia-dependent reaction), and (iii) L-glutamate oxidation in the presence of iodonitrotetrazolium salts. The NADPH oxidoreductase activity is very efficient indicating that the NADPH oxidizing site on $\beta$GltS is fully functional (*38*). On the contrary, the ammonia-dependent reaction and the glutamate:iodonitrotetrazolium oxidoreductase activities take place only at high pH values and with a low catalytic efficiency (*39*).

Glutamine hydrolysis (*i.e.*, the "glutaminase reaction") in the absence of the other substrates (namely, 2-OG and NADPH) is absent or negligible (*39, 40*). On the contrary, when 2-OG and NADPH ( or reduced Fd) are present the glutaminase and the synthase reactions are tightly coupled so that one L-Glu is formed from L-Gln and one from 2-OG (*36, 40, 41*).

The presence of the ammonia tunnel in this and other amidotrasferases raises the questions of (i) how the enzyme controls and coordinates the glutaminase and synthase activities across the tunnel, (ii) whether ammonia or ammonium ion is the transferred species, and (iii) if (and how) the protein directs the ammonia molecule from the glutaminase to the synthase site along the tunnel.

## THE AMMONIA TUNNEL

In all the well-characterized amidotransferases, the ammonia tunnel is not formed by the GAT domain, which is conserved among enzymes of the same class. Rather, it is formed by residues of the synthase domain, which are structurally and functionally unrelated to each other even in amidotransferases of the same class. This observation is leading to the proposal that amidotransferases are an example of a very sophisticated case of convergent evolution in which the ammonia tunnel is the common solution found to the problem of transferring ammonia from the site of glutamine hydrolysis to the site where the acceptor molecule is located, by avoiding its escape into the medium and, therefore, the wasteful consumption of glutamine.

The fact that the ammonia tunnel is formed by the unrelated synthase domains explains the differences in the tunnel architectures observed in these enzymes.

In αGltS the tunnel spans about 30 Å when measured from the MetS sulfur atom to the C(2) carbon of 2-OG (Fig. 2). It is actually formed by two adjacent cavities. The first one, toward the glutaminase site, is spherical in shape and is lined by residues of the glutaminase, central, and synthase domains. An obstruction formed by backbone atoms of residues 503–504 of the central domain and residues 976–977 of the synthase domain separates it from its second and main part, which is conical in shape. The latter is lined mainly by main chain carboxyl and side chain oxygen atoms and aliphatic side chains of loops 4 (residues 933–978 in αGltS) and 6 (residues 1025–1047 in

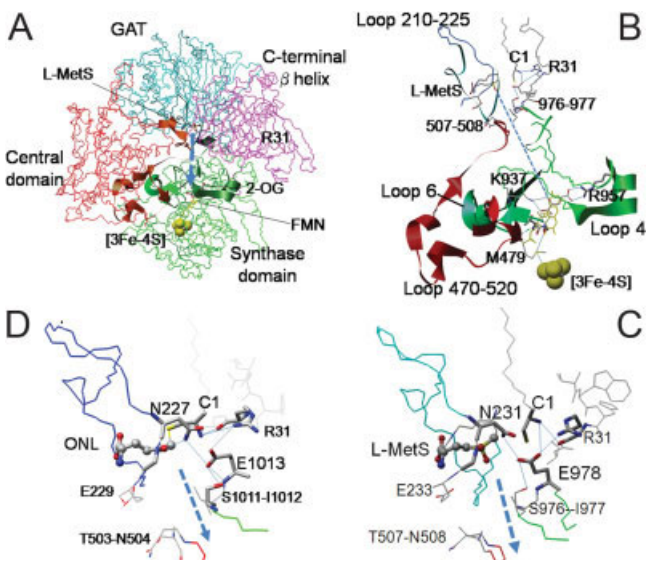


**Figure 2.** Structure of glutamate synthase. Panel A: Structure of αGltS in complex with 2-oxoglutarate (2-OG) and L-methionine sulfone (MetS) determined at 3.0 Å resolution [(*31*), PDB ID: 1ea0]. The position of MetS, 2-OG, FMN and of the [3Fe-4S] cluster are indicated. The polypeptide chain is color coded as follows: blue, glutamine amidotransferase domain (residues 1–421); red, central domain (residues 422–780), a $\beta/\alpha$ fold with high structural (but not sequence) similarity with the region comprising $\beta$ strand 1 and $\beta/\alpha$ units 5, 6, 7, and 8 of the synthase domain, a $(\beta/\alpha)_8$ barrel. A α helix connects the $\beta$ strands topologically equivalent to $\beta$1 and $\beta$6 of a $(\beta/\alpha)_8$ barrel; green, the synthase domain (residues 781–1202), a $(\beta/\alpha)_8$ barrel; magenta, the C-terminal domain (residues 1203–1472), whose core is formed by a right handed $\beta$ helix comprising seven helical turns, which spans 43 Å in length and is a fold so far unique to GltS. The terminal 7 residues of the polypeptide chain are not visible in the crystallographic structure. Panel B: Details of the core region of the protein where the intramolecular ammonia tunnel is located. The blue dotted line indicates the ~30 Å-long path of ammonia from the site of release to the C(2) atom of 2-OG in the synthase domain across the tunnel. Loop 4, residues 933–978. Loop 6, residues 1025–1047. The central domain loop 470–520 is also shown. Color code is as in panel A. Panel C: Details of the glutaminase site in αGltS in complex with MetS. Among the residues shown, C1, is the catalytic Cys residue whose side chain sulphur atom is pointing away from the expected position of L-Gln C(5) carbon, indicating an nonproductive conformation as a result of the presence of MetS. The N231 side chain amide group forms an oxyanion hole with the backbone amide hydrogen of G230, which favors glutamine hydrolysis; In blue is loop 210–225, the Q loop of amidotransferases, which is found in an open conformation. E978 is the only residue of the synthase domain making contacts with residues of the glutaminase site. The residues of loop 4 (green) and of loop 470–520 of the central domain (red), which obstruct the tunnel entrance are shown. Panel D: The residues of Fd-GltS [PDB ID: 1OFE, (*33*)] corresponding to those of αGltS shown in panel C are presented. Here the enzyme crystals were reacted with L-5-diazo-5-oxo-norleucine DON, which formed a covalent 5-oxo-norleucine (ONL) adduct with C1 thiol mimicking the γ-glutamyl-thioester reaction intermediate. In panels C and D, the blue thin lines indicate potential hydrogen bonding interactions (<3.5 Å) among active site residues, which involve E1013 of Fd-GltS (E978 in GltS) and may be relevant for coupling the synthase reaction to glutamine hydrolysis and ammonia transfer through the tunnel. This and other molecular graphics images were produced using the UCSF Chimera package from the Resource for Biocomputing, Visualization, and Informatics at the University of California, San Francisco (supported by NIH P41 RR-01081).

αGltS) of the synthase domain and the 470–520 loop of the central domain. Interesting, along the tunnel wall, several conserved Pro residues of the central (Pro 509 and 510 ) and synthase (Pro 938, 968, 969, 970) domain are found. The Pro 968–970 residues of the synthase domain are particularly interestingly in that they belong to a characteristic sequence essentially unique to GltS. Charged residues are found only at the entry (the spherical cavity toward the glutaminase site) and exit (toward the synthase site) points. Here, a salt bridge between the side chains of Glu886 and Lys931 partially obstructs the tunnel. Thus, solvent accessibility of the tunnel depends on that of the glutaminase and synthase sites and on the degree of obstruction at the entry and exit points. A virtually identical structure is observed for the tunnel in Fd-GltS, regardless of the ligation state of the catalytic subsites. Several water molecules were found hydrogen bonded to the polar oxygen atoms lining the tunnel (*32, 33*) raising the question of the protonation state of the transferred ammonia molecule.

Studies of the pH dependence of the ammonia-dependent glutamate synthase reaction catalyzed by the NADPH-GltS have been carried out (*42*). In this reaction ammonia (supplied as ammonium chloride) substitutes for L-Gln as the ammonia source for L-Glu synthesis from 2-OG. The studies showed that ammonia rather than ammonium ion is the reaction substrate. This result could be interpreted as to indicate that ammonia is the transferred species, provided that in this reaction the ammonia substrate enters the enzyme from the glutaminase site and uses the tunnel to reach the 2-OG acceptor. However, the reaction proceeds at the pH optimum of about 9.5 with a velocity that is 20–30% that of the physiological L-glutamine-dependent reaction at its pH optimum of 8, and the $K_m$ for ammonia + ammonium ion, even at the pH optimum, is very high (about 1 M). The ammonia-dependent reaction was also little sensitive to DON or iodoacetamide modification of Cys1 (*42*). These data suggest that ammonia binds to the synthase site where it reacts with 2-OG, or even that it reacts in solution with free 2-OG forming 2-IG, which is the actual species that binds to the enzyme. The hypothesis that free ammonia enters the synthase site directly rather than through the tunnel is supported by $^{15}$N-NMR spectroscopy studies (*40*). When the NADPH-GltS reaction was carried out in the presence of L-[$^{15}$N-amido]-Gln, 2-OG and NADPH, quantitative transfer of the labeled nitrogen to 2-OG to yield L-[$^{15}$N-amino]-Glu was observed with no loss of ammonia into the solvent. Furthermore, no incorporation of labeled nitrogen was observed in either L-Gln or L-Glu when the reaction was carried out in the presence of $^{15}$N-ammonium chloride and unlabeled L-Gln and 2-OG.

A similar lack of exchange of the transferred ammonia with excess ammonia from the medium was observed for PRPP-AT and GlmS (*25, 29, 30*). In CPS, ammonia is believed to bind at the synthase site in the absence of glutamine (*43, 44*). On the contrary, in AS it has been recently shown that $^{15}$N from ammonia is efficiently incorporated into glutamine in competition experiments supporting the concept that it enters the tunnel from the glutaminase site (*45*). However, AS is unique among amidotransfeases in that it uses ammonia very efficiently as the nitrogen donor, even under physiological conditions, and the glutaminase and synthase reactions are very weakly coupled.

In general, in amidotransferases it is accepted that ammonia is the transferred molecule in order to guarantee its nucleophilic character for the subsequent addition to the acceptor molecule. In support of this proposal is also the fact that in other amidotransferases (*e.g.*, PRPP-AT, GlmS, AS) the tunnel is often hydrophobic. However, in, *e.g.*, IGPS (*46, 47*) several polar residues line the tunnel and in the *Staphylococcus aureus* glutamyl-tRNA$^{Gln}$ amidotransferase, an amidotransferase of the amidase structural class (*48*), the tunnel is hydrophilic.

The question of the molecular species being transferred from the glutaminase to the synthase site has been addressed through computational studies. In the case of bacterial IGPS (*49, 50*), which is formed by a HisH subunit harboring the Type I (Triad) GAT domain and a HisF subunit, harboring the tunnel and the synthase site, the tunnel is mainly hydrophobic although a few polar groups are present and some water molecules are found in the crystallographic structures. The transfer of an ammonia molecule was found to be possibile and to require the presence of at least one water molecule to accompany it along its journey across the tunnel. The main obstacle to ammonia transfer is the gate formed by salt-bridging, conserved, positively and negatively charged residues at its entry point. However, binding of the acceptor molecule at the synthase site causes their reorientation and widens the tunnel entrance. Molecular dynamics simulations have also been performed to study the transfer of ammonia across the tunnel of GlmS (*51*). Here the tunnel is mainly hydrophobic. At its entry point, diffusion of ammonia toward the synthase site is opposed by the presence of Trp74 side chain, which obstructs the tunnel, and, mainly, interactions with the Cys1 α-amino group and Thr606 hydroxyl group. Ala602 and Val605 of the synthase domain partially obstruct the entrance of ammonia into the synthase site. Overall, ammonia is observed to migrate to the synthase site without, however, the assistance of any of the few water molecules found in the tunnel.

## COUPLING OF THE GLUTAMINASE AND SYNTHASE REACTIONS THROUGH SUBSTRATE-INDUCED CONFORMATIONAL CHANGES

The lack of relation among the synthase sites in various amidotransferases may also explain why they differ from each other with respect to the degree of coupling of glutamine hydrolysis in the amidotransferase domain and generation of the aminated (or amidated) product at the synthase site.

The degree of coupling of amidotransferases is typically evaluated by comparing the rate of formation of glutamate and ammonia from glutamine in the glutaminase domain, and the rate of formation of the aminated (or amidated) product of the synthase reaction under various conditions. Thus, a second indicator of the degree of coupling is given by the rate of glutamine

hydrolysis in the absence of the acceptor substrate, which is referred to as the glutaminase reaction. In most amidotransferases this reaction takes place at a very low rate, with often a high $K_m$ value for L-Gln. The presence of the acceptor molecule in the synthase site both increases the rate of the glutaminase reaction and ensures tight coupling so that essentially one glutamine is hydrolyzed per product of the synthase reaction being formed (*25, 29, 30*).

As a result of the acceptor-stimulated glutamine hydrolysis and the tight coupling between the glutaminase and synthase reactions, a common feature of amidotransferases is the fact that they must exist in at least two conformational states. In the free form, the glutaminase site is inactive. Binding of the acceptor at the synthase site triggers conformational changes that activate the glutaminase site and ensure coupling of the glutaminase and synthase reactions across the tunnel. The determination of the precise nature of these conformational changes, the identification of the residues implicated in signal trasmission between the sites and the estimate of the rates at which the conformational changes occur during the catalytic cycle is actively pursued for the various amidotransferases. In the light of the fact that amidotransferases are formed by conserved amidotransferase domains, which are associated to unrelated synthase domains, the nature of the activatory conformational changes, initiated by acceptor binding to the synthase site, and of the residues implicated in signal transduction differ in the different amidotransferases. However, some common features are emerging in support of the hypothesis that these enzymes are the result of a case of independent convergent evolution.

In the case of NADPH-GltS, the enzyme appears to exert a tight control over the reaction so that essentially no glutamine hydrolysis is observed when the enzyme is incubated with L-Gln alone or with L-Gln and only one of the other substrates. In the presence of 2-OG and NADPH, the same rate of L-Glu formation from L-Gln as that of L-Glu formation from 2-OG is measured with no release of ammonia into the medium nor incorporation of ammonia from the medium into glutamine or glutamate produced from 2-OG (*36, 40, 52*). Interestingly, a strong glutaminase activity is observed with the isolated αGltS indicating that a conformational change occurs within αGltS upon association with the βGltS during the enzyme biogenesis and that this event is essential to guarantee the correct cross-control of the glutaminase and synthase activities of GltS (*52*). In Fd-GltS, a glutaminase reaction is sometimes observed, but, when present, it occurs at a negligible rate (<2% that of the physiological glutamine-dependent glutamate synthase reaction) (*33, 36, 41*). The reaction is not stimulated by the presence of each one of the other substrates (2-OG and reduced Fd) when added individually (*36*). On the contrary, in the complete reaction mixture the stoichiometry of glutamine being hydrolyzed at the glutaminase site and of glutamate produced from 2-OG at the synthase site is 1:1 (*36, 41*).

These results indicate that, as in the case of other amidotransferases, GltS exists in at least two conformations. In both states, the synthase site can bind 2-OG and the cofactors can be reduced. In the conformation of the free enzyme, the glutaminase site is inactive, although it may bind glutamine as shown by the ability of DON to inactivate the enzyme in the absence of 2-OG (*42*). When 2-OG binds at the synthase site and the enzyme cofactors are in the correct redox state, a catalytically competent conformation of the glutaminase site is reached. In Fd-GltS, it has been shown that reduced Fd must be in complex with reduced enzyme to obtain the fully active enzyme (*36, 41*).

Inspection of the three-dimensional structures of αGltS and of Fd-GltS reveals the type of conformational changes that might occur during turnover and which protein segments may signal the presence of the ligands of the synthase site to the GAT domain across the ammonia tunnel.

In αGltS in complex with MetS and 2-OG, the geometry of the glutaminase site reflects a conformation, which is not catalytically competent in that (i) the Cys1 sulphur atom points away from the L-Gln binding site and (ii) loop 210–220, the Q loop of PurF-type amidotransferases, is an an open conformation exposing the glutaminase site to bulk solvent (Fig. 2C). Cys1 thiolate is required to approach L-glutamine C(5) position in order to initiate glutamine hydrolysis (Fig. 1, lower panel). The Q loop ( from "glutamine (Q) specificity" loop) has been found in a closed position in the catalytically active conformations of other amidotransferases of this class, preventing the escape of the released ammonia molecule (*23, 26, 30, 33*). The Fd-GltS structure has been solved with the unligated glutaminase site or after reaction with DON. The latter is a glutamine analog, which inactivates the enzyme as the result of the nucleophilic attack of Cys1 thiolate on its C(6) position leading to the covalent and irreversible adduct with the resulting 5-oxonorleucine (ONL). The GltS-ONL complex is a mimick of the enzyme γ-glutamyl thioester reaction intermediate (Fig. 1, lower panel, Fig. 2D). In all these structures, the Q loop is also open, but Cys1 sulphur atom is at a location compatible with glutamine hydrolysis or engaged in the covalent bond with the ONL moiety, respectively. Thus, crystallography trapped an inactive conformation of αGltS due to the presence of MetS, whose bulky sulphone group has pushed away the Cys1 side chain, but an active conformation in all Fd-GltS structures. Interestingly, as discussed in detail in (*23*), repositioning of Cys1 is accompanied by a shift of the backbone of loop 31–39 and of the preceding α helix (residues 15–30 of αGltS). As a result, changes of the interactions established by various groups in the glutaminase site are observed.

In αGltS and in Fd-GltS, regardless of the ligation state, the intramolecular tunnel is formed, but it is obstructed at its entry site (*i.e.*, toward the glutaminase site) by backbone atoms of the residues 976–977 (belonging to loop 4 of the synthase domain) and 507–508 (of loop 470–520 of the central domain) (Fig. 2). How the presence of 2-OG and reduced cofactors (and bound reduced Fd in Fd-GltS) may be sensed by the glutaminase site and the tunnel entry point is suggested by GltS structures. Loop

4 carries at its N-terminus Lys937 and Arg957 (in αGltS), which interact with 2-OG α-carboxylate and carbonyl groups, and with the δ-carboxylate, respectively, in the synthase site. After lining the tunnel, loop 4 contributes with residues 976–977 to the tunnel obstruction. Finally, with residue E978 it may make several contacts with residues of the glutaminase domain, which may be important for the glutaminase segment of the reaction. By inspecting the structure of the catalytically competent conformation of Fd-GltS, this glutamate residue (E1013 in Fd-GltS) appears to be important for positioning of Cys1 (through interactions with R31 and direct interaction with Cys1 α-amino group), and glutamine hydrolysis (through interaction with the Cys1 α-amino group and with N231 carbamide nitrogen, which is part of the oxyanion hole stabilizing the tetrahedral transient reactions intermediates with the backbone amide of Gly232). E1013 side chain carboxylate is also in contact with both its own backbone amide nitrogen and with the side chain of the Ser residue obstructing the tunnel (Ser976 in αGltS and Ser 1011 in Fd-GltS) linking the precise conformation of the tunnel entrance to that of the glutaminase site. Thus, loop 4 may sense the presence of 2-OG at the synthase site and induce activation of the glutaminase site and opening of the tunnel entrance. In this process, E978 of αGltS (E1013 in Fd-GltS) may play a pivotal role.

Loop 470–520 of the αGltS central domain may instead act as the primary sensor of the redox state of the GltS cofactors at the synthase site, adding a regulatory role to this domain to the already mentioned structural role. Met479 of this loop, the only residue of αGltS and Fd-GltS falling in a disallowed region of the Ramachandran plot, is in van der Waals contact with both FMN and the [3Fe-4S] cluster. Met479 may sense the change in the cofactors redox state and transmit it to residues 507–508 of this loop at the tunnel obstruction point, and to residues of the glutaminase domain through its C-terminal part. Furthermore, Met479 may contribute to sensing the presence of the bound 2-OG (linking the redox state of the synthase site to its ligation state) being its main chain amide nitrogen in contact with T1030 of loop 6 (residues 1025–1047), which, in turn interacts with 2-OG α-carboxylate.

In Fd-GltS, the presence of bound reduced Fd, which is required for activity, may be sensed by loop 4 through Tyr987 which is in contact with Asp907 of loop 907–933. This loop has been defined as the "Fd loop" since it corresponds to an insert found in Fd-GltS when compared with αGltS. The conservation (and role) of the "Fd loop" in Fd-GltS has been recently challenged upon studies on the enzyme from the hydrogen-oxidizing chemoautotrophic bacterium *Hydrogenobacter thermophilus* TK-6 (*53*). This enzyme is claimed to be Fd-dependent, but no insert is found.

In the GltS crystal structures, 2-OG is bound in front of FMN at a position consistent with a mechanism in which ammonia emerging from the tunnel adds to the C(2) carbon atom forming the postulated 2-IG intermediate. It is shielded from solvent by residues of loops 4 and 6. K937 of loop 4 (in αGltS) forms hydrogen bonds with the carbonyl oxygen of 2-OG, perhaps favoring ammonia addition. However, the C(2) atom of 2-OG appears to be too far from FMN N(5) position (4 Å) to allow for the reduction of 2-IG to L-Glu. Thus, after formation, repositioning of the 2-IG molecule is postulated to occur in order to bring it closer to the flavin for reduction. Interesting, it has been proposed that after repositioning the 2-IG imine might be sufficiently close to E886, and that this residues may assist its reductive conversion to L-Glu (*23*).

Thus, in a minimal scheme, it is proposed that free GltS is in a resting state unable to hydrolyze ammonia and with an obstructed tunnel entry site. Binding of 2-OG and cofactors reduction induces catalytically relevant conformational changes across the tunnel through small conformational changes of residues of loops 4 and 6 of the synthase domain and the central domain loop that activate the glutaminase reaction. This step must be accompanied by closure of the Q loop to avoid the escape of the released ammonia molecule into the medium and its protonation, as well as to direct it toward the ammonia tunnel. At the same time, conformational changes must induce the opening of the tunnel entry point to allow for ammonia transfer. At the synthase site, 2-OG is bound so that ammonia can efficiently add to its C(2) position in a nucleophilic addition promoted by K937. Once the 2-IG intermediate is formed, a rotation of the molecule anchored into the active site by interactions between its carboxylates groups and charged and polar side chains is sufficient to bring C(2) at a position that may allow its reduction by reduced FMN by direct hydride transfer. In Fd-GltS, binding of reduced Fd to the reduced enzyme may be sensed by the Fd loop and transmitted to the glutaminase site through loop 6.

## CONFORMATIONAL FLEXIBILITY OF GltS AS REVEALED BY MOLECULAR DYNAMICS SIMULATIONS

That GltS may undergo activatory conformational changes upon substrates binding and cofactors reduction has been shown by a set of molecular dynamics simulations (*54*). Models of the unligated and oxidized αGltS ($\alpha GltS_{free}$) and of a species modeled with bound L-Gln and 2-OG and reduced FMN ($\alpha GltS_{bound}$) were obtained from the crystallographic coordinates of αGltS in complex with L-MetS and 2-OG. The 4 ns simulation of $\alpha GltS_{free}$ led to the observation of a collapse of both the glutaminase and synthase sites, which become unable to bind their substrates, and to a further constriction of the tunnel entry site. The simulation of $\alpha GltS_{bound}$ led to the observation of Cys1 side chain repositioning, accompanied by that of loop 31–39 carrying Arg 31. As a result, a geometry compatible with the nucleophilic attack of L-Gln C(5), similar to that of the Fd-GltS structures, was observed. This conformational change took place with quasi-rigid body motions of well-defined segments of the glutaminase domain. Widening of the tunnel entry point was also observed. However, in the synthase site, 2-OG moved further away from the FMN N(5) position, giving no hints about

its location after conversion to the 2-IG intermediate. Interestingly, in the glutaminase site, loop 210–220 (the Q loop of amidotransferases) remained in the open conformation throughout the simulation, but another loop (residues 263–271), which is open in the crystal structure and during the simulation of the $\alpha GltS_{free}$, closed onto the glutaminase site to partially shield it from solvent suggesting that it may replace the function of loop 210–220. Interestingly, only a few water molecules are found in the tunnel of the modeled $\alpha GltS_{free}$ in spite of the solvent accessibile glutaminase site, but in agreement with the narrowing of its entry point. On the contrary, water molecules are found to fill the tunnel of the modeled complex with 2-OG and L-Gln at positions similar to those of water molecules observed in the Fd-GltS crystallographic structures. This is in agreement with the widening of the tunnel entry site and the partial solvent accessibility of the glutaminase site in spite of the closure of loop 263–271. Although the size (thus computational cost) of GltS discouraged the extension of these molecular dynamics studies, the simulations provided a possibile picture of the structure of GltS in the free (inactive) state and supported the conclusion that the crystallographic structures of Fd-GltS correspond to the catalytically active conformation of the reduced enzyme in complex with L-Gln and 2-OG. It remains to be established if the Q loop, which is observed in the open position in both the crystals and at the end of simulations, will close during the catalytic cycle, as suggested for other amidotrasnferases, or if it remains open and it is actually functionally substituted by the loop 263–271 highlighted by the computational studies.

## THE TWO-STEP ACTIVATION PROCESS OF GLUTAMATE SYNTHASE

At variance with other amidotransferases the crystallographic structures of free and 2-OG bound Fd-GltS, as well as the covalent Fd-GltS-ONL complex are similar to each other, so that it is not possible to identify conformational changes linked to enzyme reduction, binding of 2-OG and binding of L-Gln as done for, *e.g.*, PRPP-AT and, more recently, GlmS [as reviewed in (*26*)]. In these enzymes, structural studies revealed that the tunnel forms only upon binding of the ammonia acceptor substrate, which causes significant rearrangements of several protein segments. However, the finding of a fully formed tunnel is not unique to GltS. For example, a tunnel is identified in the structure of ligand free IGPS. In several cases, even when the tunnel is formed, the entry site is often obstructed as found for GltS. This is the case of IGPS conserved ring of salt-bridging residues with the "gating" Lys residue [Lys 99 in the HisF subunit of *Thermotoga marittima*, (*47*)], Trp74 of GlmS or Tyr74 of PRPP-AT (*26*).

In spite of differences in the structure and structuring of the tunnels, and of the position and nature of obstructing residues, if present, another emerging common feature of amidotransferases is the presence of one residue of the (unrelated) synthase domain making key contacts with residues of the glutaminase site, which may transmit the presence of the ammonia acceptor molecule in the synthase domain to the glutaminase site, determining its activation. For example, this residue is Thr606 in GlmS, Ile335 of the flexible loop of PRPP-AT and Tyr383 of AS, or D359 of yeast IGPS (*26, 41, 55*).

In GltS, this residue is E978 of αGltS corresponding to E1013 of Fd-GltS (Fig. 2D). The latter was replaced with D, N, and A residues, leading to proteins that exhibited dramatically lowered activity (~150-fold with respect to the wild-type protein for the D variant and 5000–10000-fold for the N and A variants, respectively, Fig. 3) (*41*). The E1013 substitution seemed to specifically affect the rate of the early steps of the glutaminase reaction, perhaps due to a specific effect on the geometry of the oxyanion hole through a change in the interaction with N227, whose γ-amide nitrogen is part of the anion hole with G228 backbone amide nitrogen (Fig. 2D). Substitution of E1013 with D and N led to two interesting observations. In the E1013N variant, the rate of glutamate produced from glutamine hydrolysis doubled that of glutamate produced from 2-OG at the synthase site (Fig. 3). This result is fully consistent with the interactions established between E1013 side chain carboxylate and Ser1011 side chain, which are likely prevented in the N1013 species, and which would couple activation of the glutaminase site and widening of the tunnel entrance upon 2-OG binding at the synthase site through loop 4 residues (Fig. 2D). The substitution of E1013 with D instead led to the unexpected finding of a sigmoid relation between initial velocity and L-glutamine concentration at high 2-OG concentrations (Fig. 3). The data could be interpreted as to indicate that the activation of the GltS glutaminase site is a two-step activation process (Fig. 4). Binding of 2-OG and cofactors reduction at the synthase site may lead to a first conformational transition leading to an inactive or poorly active glutaminase site. Binding of glutamine to this site may cause a second conformational change in its own site, which leads to fully active enzyme. Because Fd-GltS appears to be monomeric in solution, the sigmoidicity may arise from kinetic effects instead of a "classical" allosteric effect: the conformational change of the glutaminase site brought about by 2-OG binding is fast in the wild-type enzyme, leading to hyperbolic kinetics. However, it becomes slow when E1013 is substituted by D as a consequence of alteration of the transduction path. In this case, the level of the fully active species is set by the concentration of L-Gln leading to the observed sigmoid behavior, provided that the return to the initial inactive conformation is a slow process.

The two-step activation process of GltS, which involves both the "ligands" of the synthase site (*i.e.*, 2-OG and electrons) and binding of glutamine at the glutaminase site, may be a further proof of the sophisticated case of convergent evolution observed in amidotransferases. A similar two-step activation process has been proposed for PRPP-AT on the basis of the crystallographic structures of the enzyme in different ligation states and fluorescence-monitored conformational changes (*56–58*) and, recently, by comparing crystal structures of various forms of GlmS (*59*).

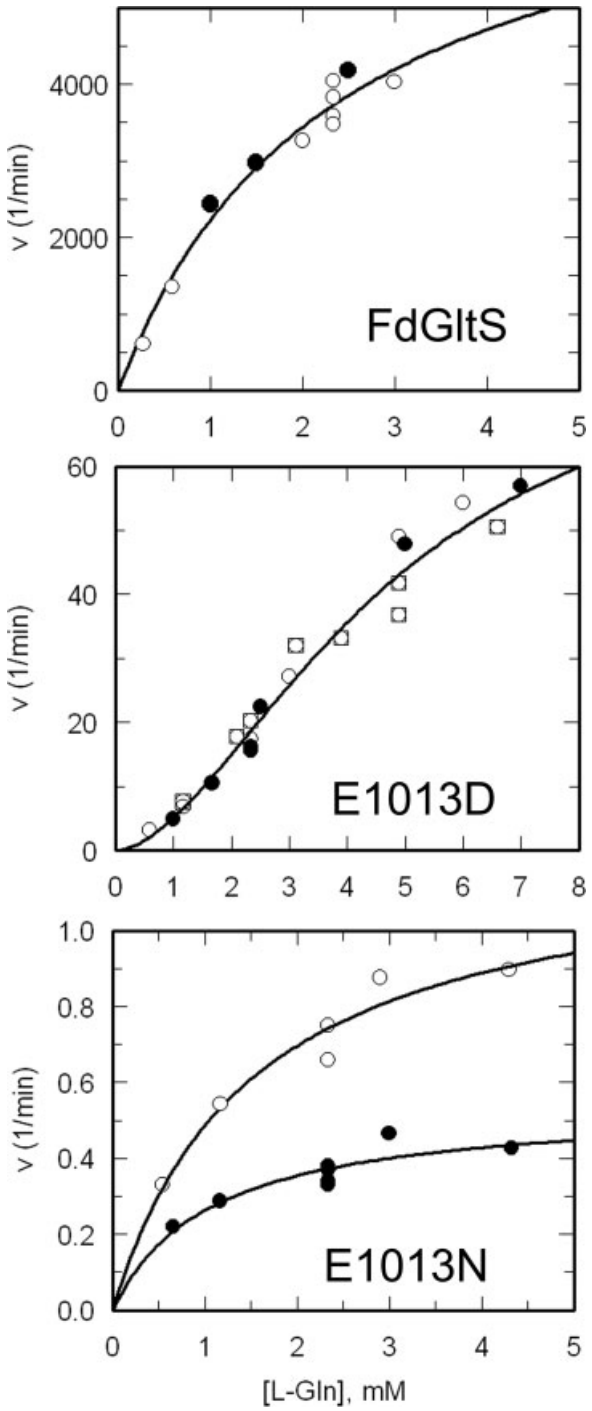


**Figure 3.** Role of E1013 of Fd-GltS in activation and coupling of glutamine hydrolysis and glutamate synthesis from 2-oxoglutarate. The panels show the dependence of the inital velocity of L-[U-$^{14}$C] glutamate formation from L-[U-$^{14}$C] glutamine (empty symbols) or 2-[U-$^{14}$C] oxoglutarate (closed symbols) catalysed by the wild-type and the E1013D and E1013N variants of Fd-GltS at 25°C, pH 7.5 and in the presence of 5 mM 2-OG, 21 $\mu$M Fd, 4 mM dithionite (*41*).

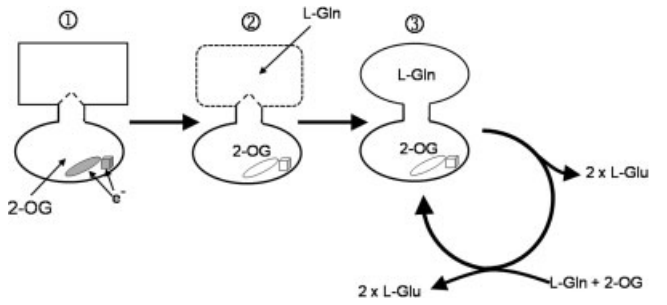


**Figure 4.** Two-step activation of glutamate synthase. It is here proposed that in the free enzyme (state 1) the synthase site is capable to bind 2-OG and accept reducing equivalents, but the glutaminase site is inactive. An obstructed ammonia tunnel is present. Binding of 2-OG and cofactors reduction at the synthase site, induces a first conformational change in the glutaminase site that is now capable to bind glutamine (state 2). A second conformational change now leads to a fully active glutaminase site and an open tunnel to allow for the transfer of ammonia to the synthase site where the reaction is completed (state 3). In the wild-type enzyme, the conversion of state 1 into state 2, which is brought about by 2-OG and reducing equivalents, is fast leading to hyperbolic kinetics. It is not known if at the end of each catalytic cycle the enzyme is ever in the free state and returns to state 1 or if it cycles in the state 3 conformation (round arrow). In the E1013D, the conversion from state 1 to state 2 has become slow and thermodynamically unfavored. If the return of the enzyme from state 3 to state 1 at the end of each catalytic cycle is slow, the concentration of the catalytically active species (state 3) is set by L-Gln concentration, which will cycle in state 3 as depicted by the round arrow, leading to the sigmoid kinetics of Fig. 3 (middle). The oval representing FMN and the cube representing the [3Fe-4S] cluster are gray when oxidized and white in the reduced state.

In this respect, it should be noted that inspection of the crystallographic structures becoming available and the growing body of information gathered by site-directed mutagenesis of various amidotransferases is indicating that this two-step activation process may take place in all amidotransferases, but also that several residues are important for signal trasmission.

## THE NADPH-GltS $\alpha\beta$ PROTOMER STRUCTURE AND THE ELECTRON TRANSFER PATH FROM FAD TO FMN

A key issue concerning NADPH-GltS is the determination of the structure of the $\alpha\beta$ protomer, which has resisted the innumerable crystallyzation attempts carried out over the past decade. Its high resolution structure might reveal the alternative conformations of the enzyme and how the glutaminase and synthase reactions are tightly coupled in the NADPH-GltS $\alpha\beta$ holoenzyme, but not in the isolated $\alpha$GltS. Furthermore, a molecular model of the $\alpha\beta$ protomer would provide information on the

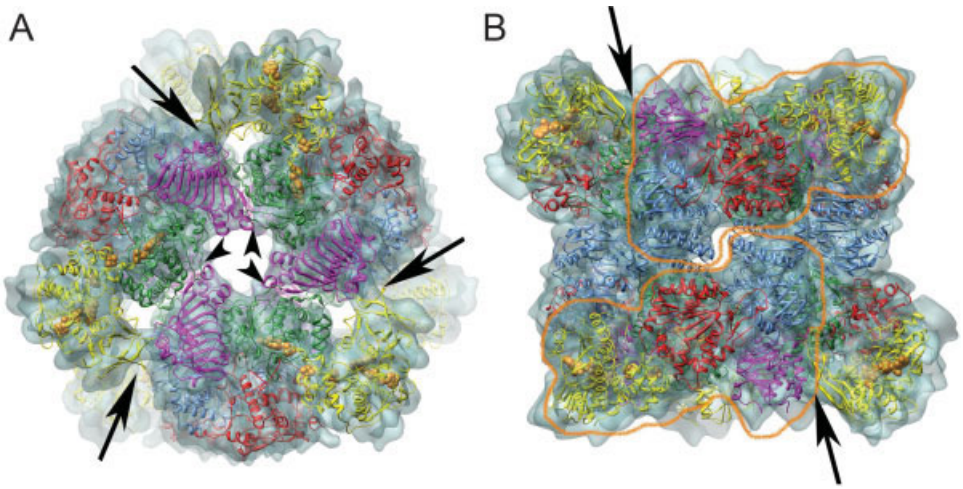


**Figure 5.** Structure of NADPH-GltS $(\alpha\beta)_6$ hexamer as derived by cryoEM and SAXS. The 9.6 Å volume reconstructed from cryoEM images was fitted by rigid-body modeling with the crystallographic αGltS dimer forming each one of the pillars of the hexamer and with homology models of the βGltS built by using the DPD N-terminal domain as the template, at the periphery (*64*). Panel A, top view of the complex; panel B, side view. αGltS is color coded as in Fig. 2. βGltS is yellow. The cofactors are in spacefill. In panel B, the two $\alpha\beta$ protomers forming one of the three pillars are highlighed with the orange contour line. The arrows indicate the interprotomeric α-β contacts; the arrow-heads show the interprotomeric α-α contacts.

structure of the βGltS and its cofactors, namely FAD at the NADPH oxidizing site and the two low potential [4Fe-4S] clusters. As a result, the intramolecular electron transfer pathway from FAD to FMN through the enzyme [Fe-S] clusters could be elucidated.

From sequence analyses, βGltS is a member of a small class of enzyme subunits or domains formed by an adrenodoxin reductase-like module carrying an N-terminal extension with the ligands of two [4Fe-4S] (*2, 60*). This protein class would make the reducing equivalents of NAD(P)H available to a second protein (or protein domain) through some (if not all) the [4Fe-4S] clusters encoded by the N-terminal Cys-rich regions. Among these βGltS-like proteins only dihydropyrimidine dehydrogenase (DPD) structure has been solved leading to the tentative identification of the ligands of the βGltS [4Fe-4S] clusters (*61*). Cys47, Cys50, Cys55, and Cys108 correspond to Cys79, 82, 87, and 140 of DPD where they form the first N-terminal cluster ($nFeS_I$ according to the DPD nomenclature). Cys 59, Cys98, Cys 104, and Glu124 of βGltS correspond to Cys91, Cys130, Cys136, and Gln156 of DPD forming the second N-terminal Fe-S cluster, $nFeS_{II}$.The presence of a noncysteinyl ligand in one of the GltS [4Fe-4S] clusters may explain the different electron paramagnetic spectroscopy signals we have observed for the two clusters as well as their different redox potentials (*37*). In NADPH-GltS, one of the [4Fe-4S] centers could be quantitatively reduced with NADPH (in the presence of a NADPH-regenerating system) and both could be reduced photochemically. The presence of a Glu residue, instead of the Gln side chain, in one of the GltS [4Fe-4S] clusters may explain, in part, the different redox properties of the GltS and DPD [Fe-S] clusters. At variance with GltS (*37*), none of the corresponding DPD clusters could be reduced even under mild denaturing conditions indicating a lower potential (*60, 62*).

Individual Ala substitution of Cys47, Cys50, Cys 55, and Cys59 of βGltS have been carried out and the protein variants have been coproduced with the native form of the αGltS (*63*). The primary aim of these studies was the obtainment of GltS forms specifically lacking one or the other [4Fe-4S] cluster of GltS, allowing the identification of their role in the intramolecular electron transfer process between the flavins. However, each one of the Cys-to-Ala subtitutions led to a βGltS form unable to associate with the α subunit suggesting that in GltS the [4Fe-4S] centers are essential to structure the N-terminal region forming the interface with αGltS and allowing the formation of a stable $\alpha\beta$ protomer. However, the presence of αGltS is in turn essential for the formation of the clusters as shown by the fact that the isolated wild-type βGltS contains the FAD cofactor, is catalytically active as a NADPH oxidoreductase, but is devoid of iron. A similar role may be played by these clusters in DPD as well as in all other enzymes containing a βGltS-like subunit or domain.

The sequence and functional similarities between βGltS and the N-terminal domain of DPD have been exploited to build a structural model of βGltS. The latter and the crystallographically determined structure of αGltS (*31*) have been used to generate a model of NADPH-GltS in combination with low temperature electron microscopy (cryoEM) and small-angle X-ray scattering (SAXS) (Fig. 5) (*64*). These two techniques have been used synergistically to establish that NADPH-GltS exists in solution as a mixture of $(\alpha\beta)_6$ hexamers in equilibrium with $\alpha\beta$

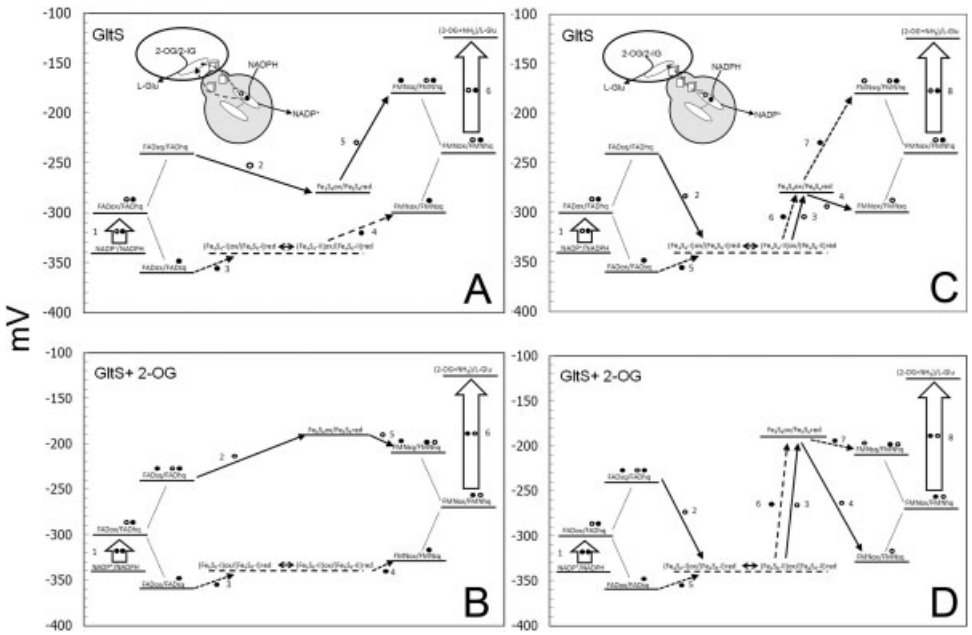


**Figure 6.** Electron transfer pathway from FAD to FMN in NADPH-GltS according to the bifurcated or linear schemes compatible with the calculated and estimated $E_m$ values of the cofactors. The $E_m$ values of the oxidized/hydroquinone forms of FAD and FMN, and of oxidized and one-electron-reduced [3Fe-4S] cluster have been determined for the free enzyme (top panels), and for the enzyme in complex with 2-oxoglutarate (2-OG, lower panels) (*35*). L-methionine sulfone (an analog of L-glutamine) and 3-amino-pyridine dinucleotide (a non reducible analog of $NADP^+$) did not alter the redox properties of the enzyme The lack of accumulation of semiquinone forms led to estimates of the $E_m$ values of the oxidized/semiquinone and semiquinone/hydroquinone couples for each one of the flavins. The two $[4Fe\text{-}4S]^{+1,+2}$ clusters of NADPH-GltS are set at a potential as low as that of the $NADP^+$/NADPH couple. Their $E_m$ values are not known, but electron spin resonance measurements showed that one can be reduced by NADPH in the presence of a regenerating system, while the other could only be reduced photochemically (*37*). With the calculated or estimated values, bifurcated (left panels) or linear (right panels) electron transfer pathways could be proposed. The sequence of the electron transfer steps is indicated by the circled numbers. The first and the second electron leaving reduced FAD are shown as empty and full circles, respectively.

protomers. The latter prevail at low protein concentration and high ionic strength. A mild dissociative effect is also brought about by the reaction product $NADP^+$, which appears to destabilize interprotomeric $\alpha$-$\beta$ contacts upon binding to $\beta$GltS (see below, and Fig. 5). Volume reconstruction based on cryoEM images and the available SAXS data allowed us to obtain an electron density map of the $(\alpha\beta)_6$ hexamer at 9.6 Å, a resolution that has been reached only recently and only in a few cases for cryoEM based structure determinations (Fig. 5). Rigid-body fitting of the $\alpha$- and $\beta$GltS atomic models in the reconstructed volume allowed to determine that the NADPH-GltS $(\alpha\beta)_6$ hexamer is better described as a trimer of $(\alpha\beta)_2$ dimers. Each $(\alpha\beta)_2$ dimer is formed by a "pillar" based on the crystallographic $\alpha_2$ dimer, the species present in the crystallographic asymmetric unit (Fig. 5B). Two copies of the $\beta$ subunit complete the two $\alpha\beta$ protomers and each of them establishes contacts with one $\alpha$GltS of the adjacent pillar (Fig. 5). These interprotomeric $\alpha$-$\beta$ contacts seem to stabilize the $(\alpha\beta)_6$ hexamer to a greater extent than interprotomeric $\alpha$-$\alpha$ contacts do. Inspection of the $(\alpha\beta)_6$ structural model showed that the C-terminal domain of $\alpha$GltS (residues 1203–1479) is essential for oligomerization. This domain is based on a right handed $\beta$ helix (residues 1226–1395) followed by three $\alpha$ helices (residues 1420–1433, 1438–1445, and 1447–1453) resting on its surface (Fig. 5). The C-terminal heptapeptide of $\alpha$GltS (residues 1473–1479) is disordered in the crystallographic structure, and its deletion was found not to influence the oligomerization state of NADPH-GltS (*64*). The N-terminal part of the $\alpha$GltS $\beta$ helical core is implicated in interprotomeric $\alpha$-$\alpha$ contacts (between $\alpha$GltS belonging to different "pillars"), by interacting with residues of the FMN domain of the adjacent $\alpha$ subunit. The $\alpha$ helices resting on its surface form the interprotomeric $\alpha$-$\beta$ interface facing residues 370–385 of $\beta$GltS of the neighboring $\alpha\beta$ protomer. Thus, the $\alpha$GltS C-terminal $\beta$ helix, which is a fold so far unique to GltS, acts as a structural spacer not only by keeping the glutaminase and the synthase domains in place, with the central domain, within $\alpha$GltS, but it also allows the formation of the GltS oligomer. As discussed previously, sequence analyses revealed that only a few proteins may contain a similar $\beta$ helical region, namely the C subunits of tungsten and molybdenum-dependent formyl metha-

nofuran dehydrogenases (Interpro classification: IPR0024889). It will be of interest to establish if these enzymes also contain a $\beta$ helix similar to that of GltS and which is its role. Indeed, this domain does not seem to be sufficient to determine oligomerization as shown by the comparison of αGltS with Fd-GltS. In the crystals of both of these proteins, the asymmetric unit is formed by similar dimers. However, Fd-GltS is a monomer in solution (*33*).

Analysis of the structure of the $(\alpha\beta)_6$ hexamer agrees with the hypothesis that the $\alpha\beta$ protomer is the minimal catalytically active unit of GltS. The fact that the enzyme, which had been preincubated in the presence of 1 M NaCl to induce its dissociation into $\alpha\beta$ protomers is catalytically active confirms this hypothesis. Interestingly, dissociation was found to be slow being completed only after 5–10 h when the enzyme (1–2 mg/ml) was incubated with 1 M NaCl. However, removal or dilution of NaCl led to reassociation of $\alpha\beta$ protomers into the hexameric species within minutes. Thus, kinetic analyses of the $\alpha\beta$ protomer had to be carried out by preincubating the enzyme in 1 M NaCl for 20 h and by carrying out assays in reaction mixtures containing 1 M NaCl, which by itself lowers $V_{max}$ by 3- to 6-fold and increased the $K_m$ values for the three substrates 10- to 100-fold. Under these conditions, dissociation of the $(\alpha\beta)_6$ hexamer into $\alpha\beta$ protomers brought about no significant change of the maximum velocity of the reaction, but a 3-fold increase of the catalytic efficiency ($V/K$) with 2-OG and L-Gln.

Inspection of the $\alpha\beta$ protomer extracted from the $(\alpha\beta)_6$ hexamer provided information on the electron transfer pathway between FAD (on $\beta$GltS) and FMN (on αGltS) along the GltS [Fe-S] clusters.

The mid-point potential ($E_m$) values of the oxidized and hydroquinone forms of the two flavins, and of the [3Fe-4S] cluster of NADPH-GltS have been determined spectrophotometrically leading also to estimates of the $E_m$ values of the flavin oxidized/semiquinone and semiquinone/hydroquinone couples (*35*). The $E_m$ values of the [4Fe-4S] centers are not known, but they have been shown to be as low (or lower) than that of the $NADP^+$/NADPH couple in that only one could be reduced with NADPH, in the presence of a regenerating system, and the other could only be reduced photochemically (*37*). Among the substrates (or their analogs) tested, only 2-OG had a dramatic effect on the $E_m$ values of the [3Fe-4S] cluster and the FMN cofactor, while association of the two subunits seemed to affect the $E_m$ value of FAD, but only to a limited extent (*35*). With the measured and calculated $E_m$ values of the various redox active species, linear or bifurcated ET pathways could be proposed (Fig. 6). The geometry of the cofactors in the model of the $\alpha\beta$ protomer of NADPH-GltS extracted from the cryoEM-derived structure (Fig. 7) indicates that the linear ET path from FAD to FMN through the two low-potential [4Fe-4S] clusters and the [3Fe-4S] center is operative. Compared with the bifurcated path, the linear scheme implies a greater number of "uphill" electron transfer steps, which are, however, possible within an overall favored oxidoreduction reaction (Fig. 6).

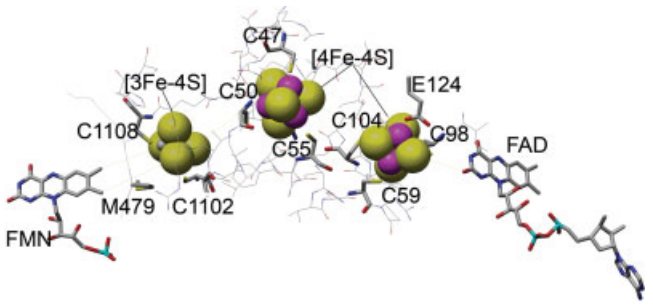


**Figure 7.** Proposed geometry of the redox centers in the NADPH-GltS $\alpha\beta$ protomer. The flavin cofactors and the three [Fe-S] clusters of GltS were extracted from that of the $\alpha\beta$ protomer reconstructed from the 9.5 Å-resolution structure of the $(\alpha\beta)_6$ hexamer obtained by cryoEM (Fig. 5) (*64*). The fourth ligand of the [4Fe-4S] cluster at the center of the image is C108, which approaches the cluster from the back side. The third cysteinyl ligand of the [3Fe-4S] cluster (C1113) is also not visible. In the [4Fe-4S] centers, which are located with FAD on $\beta$GltS, the iron atoms are purple. In the [3Fe-4S] cluster, located with FMN in αGltS, the iron atoms are gray.

## CONCLUDING REMARKS

Several aspects of GltS still need to be elucidated, and they include the exploration of the role of residues other than E978 (or E1013 in Fd-GltS) in the cross-control of the synthase and glutaminase activities. Furthermore, as discussed previously (*3*), the redox state of the catalytically active enzyme still needs to be established, and some of the protein variants being currently characterized in the laboratory may help to ask this question.

The recent cryoEM and SAXS experiments revealed that NADPH-GltS exists in solution as a $(\alpha\beta)_6$ hexamer in equilibrium with $\alpha\beta$ protomers, raising the question of the biological meaning of the reversible oligomerization behavior of the enzyme. The available information suggests that the activity of GltS is little influenced by its oligomerization state. However, it cannot be ruled out that the aggregation state affects, *in vivo*, the sensitivity of GltS to as yet unknown regulators or its ability to interact with other proteins in the cell. So far this aspect has received little attention except for the case of the spinach Fd-GltS (*65*). This species was found to copurify with UDP-sulfoquinovose synthase (SQD1), which participates in plant sulfolipid biosynthesis by adding sulfite to UDP-glucose. Interaction between tagged forms of full-length and truncated variants of Fd-GltS (used as either the "bait" or the "prey") and SQD1 could be demonstrated by affinity chromatography. Because the FMN cofactor can form an adduct with sulfite, it has been proposed that GltS moonlights as a sulfite reservoir for SQD1 and that sulfite is channeled from the GltS synthase domain to the SQD1 active center. This hypothesis is challenged by the fact that the $K_d$ for the Fd-GltS-sulfite complex is in the mM range, and the adduct is readily displaced by 2-OG, which in turn exhibits a $K_d$ in the low $\mu$M range (*36*). Thus, the fraction of

GltS in complex with sulfite in the cell is most likely negligible in the absence of modulation of its properties through protein–protein interaction.

However, in the light of the essential role of GltS in cells and of the increasing interest in this enzyme, which may be a valid target of inhibitors or metabolic engineering experiments, the search for interactors in various cell types is worthwhile and may reveal other interesting aspects of this complex enzyme.

## ACKNOWLEDGEMENTS

This work has been carried out with funds from the Ministero dell'Universita' e della Ricerca Scientifica (Rome, Italy), grants PRIN-Cofin 2003 and 2005 and FIRST 2005-2006.

## REFERENCES

1. Knaff, D. B. and Hirasawa, M. (1991) Ferredoxin-dependent chloroplast enzymes, *Biochim. Biophys. Acta* **1056**, 93–125.
2. Vanoni, M. A. and Curti, B. (1999) Glutamate synthase: a complex iron-sulfur flavoprotein, *Cell. Mol. Life Sci.* **55**, 617–638.
3. Vanoni, M. A., and Curti, B. (2005) Structure–function studies on the iron-sulfur flavoenzyme glutamate synthase: an unexpectedly complex self-regulated enzyme, *Arch. Biochem. Biophys.* **433**, 193–211.
4. Vanoni, M. A., Dossena, L., van den Heuvel, R. H., and Curti, B. (2005) Structure–function studies on the complex iron-sulfur flavoprotein glutamate synthase: the key enzyme of ammonia assimilation, *Photosynth. Res.* **83**, 219–238.
5. Drews, M., Doverskog, M., Ohman, L., Chapman, B. E., Jacobsson, U., Kuchel, P. W., and Haggstrom, L. (2000) Pathways of glutamine metabolism in *Spodoptera frugiperda* (Sf9) insect cells: evidence for the presence of the nitrogen assimilation system, and a metabolic switch by 1H/15N NMR, *J. Biotechnol.* **78**, 23–37.
6. Scaraffia, P. Y., Isoe, J., Murillo, A., and Wells, M. A. (2005) Ammonia metabolism in *Aedes aegypti*, *Insect Biochem. Mol. Biol.* **35**, 491–503.
7. Scaraffia, P. Y., Zhang, Q., Wysocki, V. H., Isoe, J., and Wells, M. A. (2006) Analysis of whole body ammonia metabolism in *Aedes aegypti* using [$^{15}$N]-labeled compounds and mass spectrometry, *Insect Biochem. Mol. Biol.* **36**, 614–622.
8. Dincturk, H. B. and Knaff, D. B. (2000) The evolution of glutamate synthase, *Mol. Biol. Rep.* **27**, 141–148.
9. Nesbo, C. L., L'Haridon, S., Stetter, K. O., and Doolittle, W. F. (2001) Phylogenetic analyses of two "archaeal" genes in *Thermotoga maritima* reveal multiple transfers between archaea and bacteria, *Mol. Biol. Evol.* **18**, 362–375.
10. Temple, S. J., Vance, C. P., and Gantt, J. S. (1998) Glutamate synthase and nitrogen assimilation, *Trends Plant Sci.* **3**, 51–56.
11. Tempest, D. W., Meers, J. L., and Brown, C. M. (1970) Synthesis of glutamate in *Aerobacter aerogenes* by a hitherto unknown route, *Biochem. J.* **117**, 405–407.
12. Miflin, B. J., Wallsgrove, R. M., and Lea, P. J. (1981) Glutamine metabolism in higher plants, *Curr. Top. Cell. Regul.* **20**, 1–43.
13. Lamichhane, G., Zignol, M., Blades, N. J., Geiman, D. E., Dougherty, A., Grosset, J., Broman, K. W., and Bishai, W. R. (2003) A postgenomic method for predicting essential genes at subsaturation levels of mutagenesis: application to *Mycobacterium tuberculosis*, *Proc. Natl. Acad. Sci. USA* **100**, 7213–7218.
14. Nandineni, M. R., Laishram, R. S., and Gowrishankar, J. (2004) Osmosensitivity associated with insertions in *arg*P (*ici*A) or *gln*E in glutamate synthase-deficient mutants of *Escherichia coli*, *J. Bacteriol.* **186**, 6391–6399.
15. Natera, V., Sobrevals, L., Fabra, A., and Castro, S. (2006) Glutamate is involved in acid stress response in *Bradyrhizobium* sp. SEMIA 6144 (*Arachis hypogaea* L.) microsymbiont, *Curr. Microbiol.* **53**, 479–482.
16. Chagneau, C. and Saier, M. H., Jr. (2004) Biofilm-defective mutants of *Bacillus subtilis*, *J. Mol. Microbiol. Biotechnol.* **8**, 177–188.
17. Kong, Q. X., Cao, L. M., Zhang, A. L., and Chen, X. (2007) Overexpressing GLT1 in *gpd*1Δ mutant to improve the production of ethanol of *Saccharomyces cerevisiae*, *Appl. Microbiol. Biotechnol.* **73**, 1382–1386.
18. Brandes, N., Rinck, A., Leichert, L. I., and Jakob, U. (2007) Nitrosative stress treatment of *E. coli* targets distinct set of thiol-containing proteins, *Mol. Microbiol.* **66**, 901–914.
19. Irazusta, V., Cabiscol, E., Reverter-Branchat, G., Ros, J., and Tamarit, J. (2006) Manganese is the link between frataxin and iron-sulfur deficiency in the yeast model of Friedreich ataxia, *J. Biol. Chem.* **281**, 12227–12232.
20. Touraine, B., Boutin, J. P., Marion-Poll, A., Briat, J. F., Peltier, G., and Lobreaux, S. (2004) Nfu2: a scaffold protein required for [4Fe-4S] and ferredoxin iron-sulphur cluster assembly in *Arabidopsis* chloroplasts, *Plant J.* **40**, 101–111.
21. Jonic, S., Sorzano, C. O., Cottevieille, M., Larquet, E., and Boisset, N. (2007) A novel method for improvement of visualization of power spectra for sorting cryo-electron micrographs and their local areas, *J. Struct. Biol.* **157**, 156–167.
22. van Breukelen, B., Barendregt, A., Heck, A. J., and van den Heuvel, R. H. (2006) Resolving stoichiometries and oligomeric states of glutamate synthase protein complexes with curve fitting and simulation of electrospray mass spectra, *Rapid Commun. Mass Spectrom.* **20**, 2490–2496.
23. van den Heuvel, R. H., Curti, B., Vanoni, M. A., and Mattevi, A. (2004) Glutamate synthase: a fascinating pathway from L-glutamine to L-glutamate, *Cell. Mol. Life Sci.* **61**, 669–681.
24. Huang, X., Holden, H. M., and Raushel, F. M. (2001) Channeling of substrates and intermediates in enzyme-catalyzed reactions, *Annu. Rev. Biochem.* **70**, 149–180.
25. Massiere, F. and Badet-Denisot, M. A. (1998) The mechanism of glutamine-dependent amidotransferases, *Cell. Mol. Life Sci.* **54**, 205–222.
26. Mouilleron, S. and Golinelli-Pimpaneau, B. (2007) Conformational changes in ammonia-channeling glutamine amidotransferases, *Curr. Opin. Struct. Biol.* **17**, 653–664.
27. Raushel, F. M., Thoden, J. B., and Holden, H. M. (1999) The amidotransferase family of enzymes: molecular machines for the production and delivery of ammonia, *Biochemistry* **38**, 7891–7899.
28. Raushel, F. M., Thoden, J. B., and Holden, H. M. (2003) Enzymes with molecular tunnels, *Acc. Chem. Res.* **36**, 539–548.
29. Zalkin, H. (1993) The amidotransferases, *Adv. Enzymol. Relat. Areas Mol. Bio.* **66**, 203–309.
30. Zalkin, H. and Smith, J. L. (1998) Enzymes utilizing glutamine as an amide donor, *Adv. Enzymol. Relat. Areas Mol. Biol.* **72**, 87–144.
31. Binda, C., Bossi, R. T., Wakatsuki, S., Arzt, S., Coda, A., Curti, B., Vanoni, M. A., and Mattevi, A. (2000) Cross-talk and ammonia channeling between active centers in the unexpected domain arrangement of glutamate synthase, *Structure Fold. Des.* **8**, 1299–1308.
32. van den Heuvel, R. H., Ferrari, D., Bossi, R. T., Ravasio, S., Curti, B., Vanoni, M. A., Florencio, F. J., and Mattevi, A. (2002) Structural studies on the synchronization of catalytic centers in glutamate synthase, *J. Biol. Chem.* **277**, 24579–24583.
33. van den Heuvel, R. H., Svergun, D. I., Petoukhov, M. V., Coda, A., Curti, B., Ravasio, S., Vanoni, M. A., and Mattevi, A. (2003) The active conformation of glutamate synthase and its binding to ferredoxin, *J. Mol. Biol.* **330**, 113–128.
34. Weeks, A., Lund, L., and Raushel, F. M. (2006) Tunneling of intermediates in enzyme-catalyzed reactions, *Curr. Opin. Chem. Biol.* **10**, 465–472.
35. Ravasio, S., Curti, B., and Vanoni, M. A. (2001) Determination of the midpoint potential of the FAD and FMN flavin cofactors and of the 3Fe-4S cluster of glutamate synthase, *Biochemistry* **40**, 5533–5541.

36. Ravasio, S., Dossena, L., Martin-Figueroa, E., Florencio, F. J., Mattevi, A., Morandi, P., Curti, B., and Vanoni, M. A. (2002) Properties of the recombinant ferredoxin-dependent glutamate synthase of *Synechocystis* PCC6803. Comparison with the *Azospirillum brasilense* NADPH-dependent enzyme and its isolated α subunit, *Biochemistry* **41**, 8120–8133.
37. Vanoni, M. A., Edmondson, D. E., Zanetti, G., and Curti, B. (1992) Characterization of the flavins and the iron-sulfur centers of glutamate synthase from *Azospirillum brasilense* by absorption, circular dichroism, and electron paramagnetic resonance spectroscopies, *Biochemistry* **31**, 4613–4623.
38. Vanoni, M. A., Verzotti, E., Zanetti, G., and Curti, B. (1996) Properties of the recombinant $\beta$ subunit of glutamate synthase, *Eur. J. Biochem.* **236**, 937–946.
39. Vanoni, M. A., Nuzzi, L., Rescigno, M., Zanetti, G., and Curti, B. (1991) The kinetic mechanism of the reactions catalyzed by the glutamate synthase from *Azospirillum brasilense*, *Eur. J. Biochem.* **202**, 181–189.
40. Vanoni, M. A., Edmondson, D. E., Rescigno, M., Zanetti, G., and Curti, B. (1991) Mechanistic studies on *Azospirillum brasilense* glutamate synthase, *Biochemistry* **30**, 11478–11484.
41. Dossena, L., Curti, B., and Vanoni, M. A. (2007) Activation and coupling of the glutaminase and synthase reaction of glutamate synthase is mediated by E1013 of the ferredoxin-dependent enzyme, belonging to loop 4 of the synthase domain, *Biochemistry* **46**, 4473–4485.
42. Vanoni, M. A., Accornero, P., Carrera, G., and Curti, B. (1994) The pH-dependent behavior of catalytic activities of *Azospirillum brasilense* glutamate synthase and iodoacetamide modification of the enzyme provide evidence for a catalytic Cys-His ion pair, *Arch. Biochem. Biophys.* **309**, 222–230.
43. Guy, H. I. and Evans, D. R. (1997) Trapping an activated conformation of mammalian carbamyl-phosphate synthetase, *J. Biol. Chem.* **272**, 19906–19912.
44. Guy, H. I., Rotgeri, A., and Evans, D. R. (1997) Activation by fusion of the glutaminase and synthetase subunits of *Escherichia coli* carbamyl-phosphate synthetase, *J. Biol. Chem.* **272**, 19913–19918.
45. Li, K. K., Beeson, W. T. t., Ghiviriga, I., and Richards, N. G. (2007) A convenient gHMQC-based NMR assay for investigating ammonia channeling in glutamine-dependent amidotransferases: studies of *Escherichia coli* asparagine synthetase B, *Biochemistry* **46**, 4840–4849.
46. Chaudhuri, B. N., Lange, S. C., Myers, R. S., Chittur, S. V., Davisson, V. J., and Smith, J. L. (2001) Crystal structure of imidazole glycerol phosphate synthase: a tunnel through a $(\beta/\alpha)_8$ barrel joins two active sites, *Structure* **9**, 987–997.
47. Douangamath, A., Walker, M., Beismann-Driemeyer, S., Vega-Fernandez, M. C., Sterner, R., and Wilmanns, M. (2002) Structural evidence for ammonia tunneling across the $(\beta/\alpha)_8$ barrel of the imidazole glycerol phosphate synthase bienzyme complex, *Structure* **10**, 185–193.
48. Nakamura, A., Yao, M., Chimnaronk, S., Sakai, N., and Tanaka, I. (2006) Ammonia channel couples glutaminase with transamidase reactions in GatCAB, *Science* **312**, 1954–1958.
49. Amaro, R. and Luthey-Schulten, Z. (2004) Molecular dynamics simulations of substrate channeling through an $\alpha$-$\beta$ barrel protein, *Chem. Phys.* **307**, 147–155.
50. Amaro, R., Tajkhorshid, E., and Luthey-Schulten, Z. (2003) Developing an energy landscape for the novel function of a $(\beta/\alpha)_8$ barrel: ammonia conduction through HisF, *Proc. Natl. Acad. Sci. USA* **100**, 7599–7604.
51. Floquet, N., Mouilleron, S., Daher, R., Maigret, B., Badet, B., and Badet-Denisot, M. A. (2007) Ammonia channeling in bacterial glucosamine-6-phosphate synthase (Glms): molecular dynamics simulations and kinetic studies of protein mutants, *FEBS Lett.* **581**, 2981–2987.
52. Vanoni, M. A., Fischer, F., Ravasio, S., Verzotti, E., Edmondson, D. E., Hagen, W. R., Zanetti, G., and Curti, B. (1998) The recombinant α subunit of glutamate synthase: spectroscopic and catalytic properties, *Biochemistry* **37**, 1828–1838.
53. Kameya, M., Ikeda, T., Nakamura, M., Arai, H., Ishii, M., and Igarashi, Y. (2007) A novel ferredoxin-dependent glutamate synthase from the hydrogen-oxidizing chemoautotrophic bacterium *Hydrogenobacter thermophilus* TK-6, *J. Bacteriol.* **189**, 2805–2812.
54. Coiro, V. M., Di Nola, A., Vanoni, M. A., Aschi, M., Coda, A., Curti, B., and Roccatano, D. (2004) Molecular dynamics simulation of the interaction between the complex iron-sulfur flavoprotein glutamate synthase and its substrates, *Protein. Sci.* **13**, 2979–2991.
55. Myers, R. S., Amaro, R. E., Luthey-Schulten, Z. A., and Davisson, V. J. (2005) Reaction coupling through interdomain contacts in imidazole glycerol phosphate synthase, *Biochemistry* **44**, 11974–11985.
56. Bera, A. K., Chen, S., Smith, J. L., and Zalkin, H. (1999) Interdomain signaling in glutamine phosphoribosylpyrophosphate amidotransferase, *J. Biol. Chem.* **274**, 36498–36504.
57. Bera, A. K., Smith, J. L., and Zalkin, H. (2000) Dual role for the glutamine phosphoribosylpyrophosphate amidotransferase ammonia channel. Interdomain signaling and intermediate channeling, *J. Biol. Chem.* **275**, 7975–7979.
58. Chen, S., Burgner, J. W., Krahn, J. M., Smith, J. L., and Zalkin, H. (1999) Tryptophan fluorescence monitors multiple conformational changes required for glutamine phosphoribosylpyrophosphate amidotransferase interdomain signaling and catalysis, *Biochemistry* **38**, 11659–11669.
59. Mouilleron, S., Badet-Denisot, M. A., and Golinelli-Pimpaneau, B. (2006) Glutamine binding opens the ammonia channel and activates glucosamine-6P synthase, *J. Biol. Chem.* **281**, 4404–4412.
60. Rosenbaum, K., Jahnke, K., Curti, B., Hagen, W. R., Schnackerz, K. D., and Vanoni, M. A. (1998) Porcine recombinant dihydropyrimidine dehydrogenase: comparison of the spectroscopic and catalytic properties of the wild-type and C671A mutant enzymes, *Biochemistry* **37**, 17598–17609.
61. Dobritzsch, D., Schneider, G., Schnackerz, K. D., and Lindqvist, Y. (2001) Crystal structure of dihydropyrimidine dehydrogenase, a major determinant of the pharmacokinetics of the anti-cancer drug 5-fluorouracil, *EMBO J.* **20**, 650–660.
62. Hagen, W. R., Vanoni, M. A., Rosenbaum, K., and Schnackerz, K. D. (2000) On the iron-sulfur clusters in the complex redox enzyme dihydropyrimidine dehydrogenase, *Eur. J. Biochem.* **267**, 3640–3646.
63. Agnelli, P., Dossena, L., Colombi, P., Mulazzi, S., Morandi, P., Tedeschi, G., Negri, A., Curti, B., and Vanoni, M. A. (2005) The unexpected structural role of glutamate synthase $[4Fe\text{-}4S]^{(+1,+2)}$ clusters as demonstrated by site-directed mutagenesis of conserved C residues at the N-terminus of the enzyme beta subunit, *Arch. Biochem. Biophys.* **436**, 355–366.
64. Cottevieille, M., Larquet, E., Jonic, S., Petoukhov, M. V., Caprini, G., Paravisi, S., Svergun, D. I., Vanoni, M. A., and Boisset, N. (2008) The subnanometer resolution structure of the 1.2 MDa glutamate synthase complex by cryo-electron microscopy and its oligomerization state in solution: functional implications. *J. Biol. Chem.* **283**, 8237–8249.
65. Shimojima, M., Hoffmann-Benning, S., Garavito, R. M., and Benning, C. (2005) Ferredoxin-dependent glutamate synthase moonlights in plant sulfolipid biosynthesis by forming a complex with SQD1, *Arch. Biochem. Biophys.* **436**, 206–214.